ELSEVIER

www.elsevier.nl/locate/jorganchem

Journal of Organometallic Chemistry 609 (2000) 83–88

Journal of Organometallic Chemistry

Bridging-terminal exchange in *ansa*-bridged tetrahydroborate niobocene compounds: a density functional study

Nicholas J. Ashworth, Stephen L.J. Conway, Jennifer C. Green *, Malcolm L.H. Green

Inorganic Chemistry Laboratory, University of Oxford, South Parks Road, Oxford OX1 3QR, UK

Received 20 April 2000; received in revised form 7 June 2000

Abstract

Density functional calculations on $[Nb(\eta\text{-}C_5H_5)_2(\eta^2\text{-}BH_4)]$, $[Nb\{H_2Si(\eta\text{-}C_5H_4)_2\}(\eta^2\text{-}BH_4)]$ and $[Nb\{H_2C(\eta\text{-}C_5H_4)_2\}(\eta^2\text{-}BH_4)]$, show the barrier to terminal-bridging hydrogen exchange decrease as the inter-ring angle increases, in agreement with earlier experimental data. The calculations suggest the bonding of BH_4 weakens as the metallocene unit becomes more bent, and that there is stronger bonding in the transition state as the d_{yz} orbital becomes more accessible. © 2000 Elsevier Science S.A. All rights reserved.

Keywords: Molecular orbital; Borohydride; *Ansa*-ligands; Terminal-bridge hydride exchange

1. Introduction

The changes in reactivity of a metallocene derivative caused by linking the two rings by a bridge may be subtle or profound [1–5]. They have become known by the generic term of *ansa*-effects. The most direct consequence of an *ansa*-bridge is to constrain the metallocene geometry and the ring rotation. The dimensions of the *ansa*-bridge can be altered to hold the rings at a fixed inter-ring angle. Typically the angle between the ring planes, α, increases along the series of bridges:

$$\text{No bridge} \sim (CH_2)_3 < (CH_2)_2 \sim SiMe_2 < CMe_2$$

The increase of angle α makes one side of the metal more sterically accessible. Introduction of an *ansa*-bridge may affect the reactivity compared to the unbridged analogue, an example being the elimination of methane from $[W(\eta\text{-}C_5H_5)_2MeH]$ contrasting with the markedly higher thermal stability of $[W\{CMe_2(\eta\text{-}C_5H_4)_2\}MeH]$ [5].

Recently the presence of an *ansa*-bridge has been found to affect the rate of exchange between bridging and terminal hydrogens in the series of tetrahydroborate niobium metallocenes, $[Nb\{X(C_5H_4)_2\}(\eta^2\text{-}BH_4)]$, where $X = CMe_2 > SiMe_2 > (CMe_2)_2$ [6]. It is well known that the bonding mode in the tetrahydroborate metal fragment may vary from η^1-H to η^3-H, with the most common bonding being that of the bidentate M-η^2-BH_4 ligation. NMR studies on η^2-BH_4 compounds often show that exchange of terminal and bridging hydrides is so rapid that only a single resonance is observed in the hydrogens ^{1}H-NMR at accessible temperatures. However, when the metal centre has a non-cylindrical electronic environment, as is the case with the niobium metallocenes, exchange is slower, and on cooling, the single resonance in the NMR spectrum broadens and separates into two bands of equal intensity due to two terminal and two bridging hydrogens. The $\Delta G^{\ddagger}$ at the coalescence temperature can be calculated and shows that as the inter-ring angle α increases the rate of exchange also increases [6].

Density functional calculations have proved very successful in reproducing changes in structure and reactivity found on introduction of an *ansa*-bridge [2,7–9]. The aim of this work was to model the exchange process in a series of tetrahydroborate niobocenes in an attempt to identify the factors underlying the structure–activity relationship described above.

* Corresponding author. Fax: +44-1865-272690.
E-mail address: jennifer.green@chem.ox.ac.uk (J.C. Green).

0022-328X/00/$ - see front matter © 2000 Elsevier Science S.A. All rights reserved.
PII: S0022-328X(00)00378-8

2. Computational methods

Calculations were performed using density functional methods of the Amsterdam Density Functional Package (Version 2.3 and 1999.02) [10,11]. Type IV basis sets used triple-ξ accuracy sets of Slater type orbitals, with a single polarization function added to main group atoms; 2p on hydrogen, and 3d on boron and carbon. The cores of the atoms were frozen; carbon up to 1s, boron up to 1s, and niobium up to 3d. First order relativistic corrections were made to the cores of all atoms. The generalized gradient approximation (GCA non-local) method was used, using Vosko, Wilk and Nusair's local exchange correlation [12], with non-local exchange corrections by Becke [13], and non-local correlation corrections by Perdew [14,15]. Frequency calculations were carried out to test that the optimized structures were local minima and that the proposed transition states were characterized by one imaginary frequency.

Reaction pathways were modeled by stepping a reaction coordinate through a sequence of fixed values and allowing the other structural parameters to optimize. These are referred to subsequently as linear transit runs.

Fragment analysis was carried out on the compounds. The molecular orbitals were first calculated for the metallocene cation and the tetrahydroborate anion as fragments. In all cases the structure of the fragment taken is that in the optimized structure of the complex. The orbitals of the tetrahydoboratometallocene molecule were then calculated using the fragment orbitals as the basis set. This enabled ready comparison of electronic structure within the series of compounds and the results were used for the construction of MO diagrams.

3. Results and discussion

The molecules chosen for theoretical calculations were unbridged (**1a**); Si bridged (**2a**); and C bridged (**3a**); niobocene borohydrides. **2a** and **3a** differ from the complexes studied experimentally, **2b** and **3b**, in that the Me substituents on the bridging atom are replaced by hydrogens (Scheme 1). This choice was made for computational simplicity since replacement of Me by H has been shown in other studies not to significantly affect structure or reactivity at the metal center [7,8].

3.1. Ground state structures

The molecular structures determined by X-ray crystallography [6,16] confirm the assignment of a bidentate η^2-BH_4 binding mode. They were used as the starting points for geometry optimizations of **1a**, **2a** and **3a**, which were carried out with the constraint of C_{2v} symmetry. Frequency calculations on the optimized structures revealed only positive frequencies confirming that they were each a local minimum.

Selected interatomic distances and angles for the optimized structures are given in Table 1 where they are compared with experimental values found by X-ray crystallography for **1a** [16], **2b** and **3b** [6]. Agreement between the calculated and experimental values for metal carbon and metal boron distances and the inter-

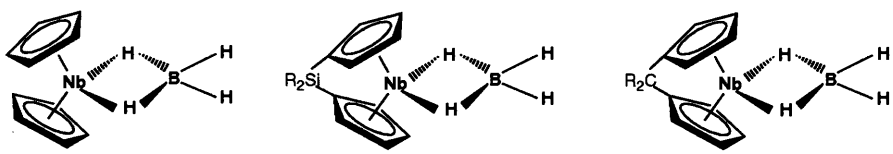

1a **2a R=H, 2b R=Me** **3a R=H, 3b R=Me**

Scheme 1.

Table 1
Selected interatomic distances (Å) and angles (°) for the compounds **1a**, **1b**, **2a**, **2b**, **3a**, and **3b**

Compound	**1a** calc.	**1a** exp.	**2a** calc.	**2b** exp.	**3a** calc.	**3b** exp
Nb–Cp^1_{ave}	2.35	2.36	2.36	2.365(4)	2.33	2.342(5)
Nb–Cp^2_{ave}	2.35	2.36	2.36	2.367(3)	2.33	2.342(5)
Nb–$H_{a,b}$	1.90	2.00	1.90	1.92(5)	1.92	1.94(7)
Nb–B	2.32	2.26	2.32	2.373	2.34	2.36(1)
B–$H_{a,b}$	1.35	1.1	1.32	1.24(5)	1.32	1.25(7)
B–$H_{c,d}$	1.21	1.1	1.21	1.11(3)	1.21	1.07(6)
α	44	50	51	53	64	65.9
H_a–Nb–H_b	71	56	70	62.0(20)	69	64.0(42)
H_c–B–H_d	110	122	110	109.6(35)	110	110.4(67)

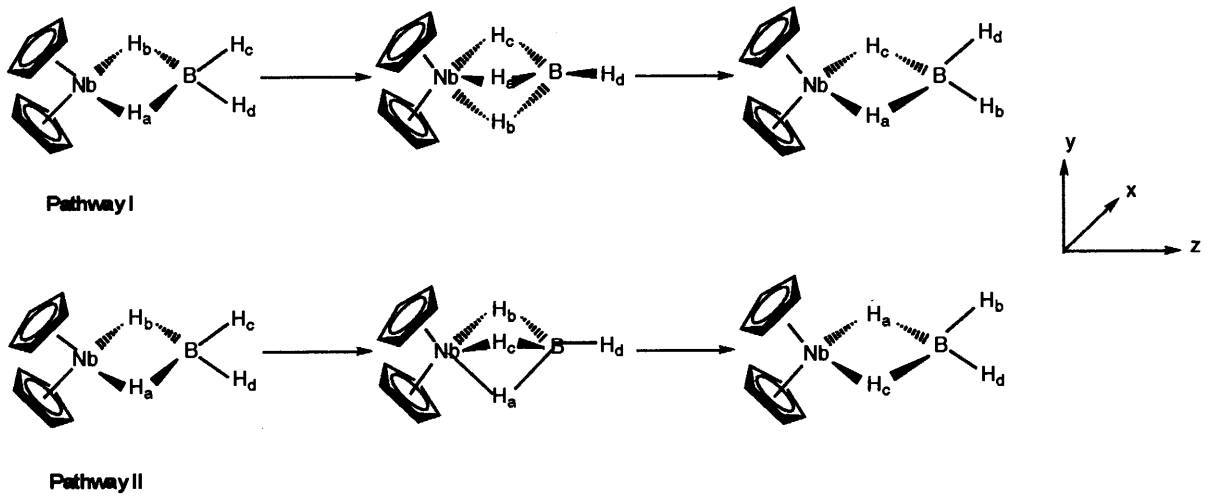

Fig. 1. Two mechanisms for bridging terminal hydrogen exchange in the niobocene η^2-borohydrides.

ring angle, α, is good. The differences in the Nb–H and B–H distances are explicable when the high standard deviations on the experimental values are taken into account, given that the problem of locating the position of hydrogen nuclei by X-ray diffraction is well known, especially in the presence of a heavy atom such as niobium.

The most substantial change along the series is the increase in α from 44° in **1a** to 64° in **3a**. The increase in bending is accompanied by a small decrease in metal-ring distance and small increases in metal borohydride distances. The size of these changes border on significance but are noted here as a similar trend was found for the series $[W\{X(\eta\text{-}C_5H_4)_2\}H_3]^+$ ($X = H_2$, SiH_2, CH_2) [8]. There is evidence that, in these d^2 systems, as α increases, bonding to the rings is strengthened and bonding to other ligands is weakened. The small changes calculated here appear to be a further example of this effect.

3.2. Mechanisms for terminal-bridging B–H exchange

Interchange of terminal and bridging hydrogens may be achieved in a number of ways [17]. Two pathways are represented diagramatically in Fig. 1. At the mid-point of the exchange reaction the interchanging hydrogens (H_b and H_c in both mechanisms) must be in equivalent positions. This is ensured in pathway 1, which describes rotation about the B–H_a bond, by the presence of xz as a mirror plane, and in pathway 2 (rotation about B–H_d) by the presence of yz as a mirror plane. It should be noted that in pathway 1, H_a stays in the same position, whereas in pathway 2, H_d remains in the same location.

A possible mid-point for pathway 1 was located by optimizing the three molecules with a C_s symmetry constraint with xz as the mirror plane. H_b and H_c were equivalent and H_a and H_d lay in the mirror plane. The resulting structures were good candidates for transition states for the exchange as frequency calculations showed them all to have one imaginary frequency. The values were 431i cm^{-1} for **1a**, 396i cm^{-1} for **2a**, and 297i cm^{-1} for **3a**. In each case the motion corresponded to rotation of the BH_4 group about the B–H_a bond as envisaged in pathway 1 (Fig. 1). Subsequent linear transit runs (see computational methods) linking these C_s structures with the ground state C_{2v} structures showed the mid-point of the exchange to be a maximum on the energy profile. The energy difference between the ground and transition states in each case is given in Table 2. Agreement with the experimental values for $\Delta G^{\ddagger}$ is good, making this pathway an excellent candidate for the exchange process. The Nb–H and B–H distance in the transition states are also given in Table 2. These suggest that whereas H_a remains strongly bound to Nb having a short Nb–H distance and a lengthened B–H distance, H_b and H_c are only weakly bound. The Nb–H bond lengths show a definite trend in the series with the Nb–H_a distance increasing with inter-ring angle α and the Nb–$H_{b,c}$ distances decreasing. Thus the difference between them is smallest

Table 2
Energies (kJ mol^{-1}) and selected distances (Å) for proposed transition states for pathway 1

Property	1a	2a	3a
Calc. energy above ground state	64.1	52.1	35.4
Experimental $\Delta G^{\ddagger}$	61.0	51.5	35.0
Nb–H_a	1.931	1.935	1.956
Nb–$H_{b,c}$	2.258	2.204	2.176
B–H_a	1.328	1.328	1.319
B–$H_{b,c}$	1.227	1.230	1.236
B–H_d	1.204	1.202	1.202

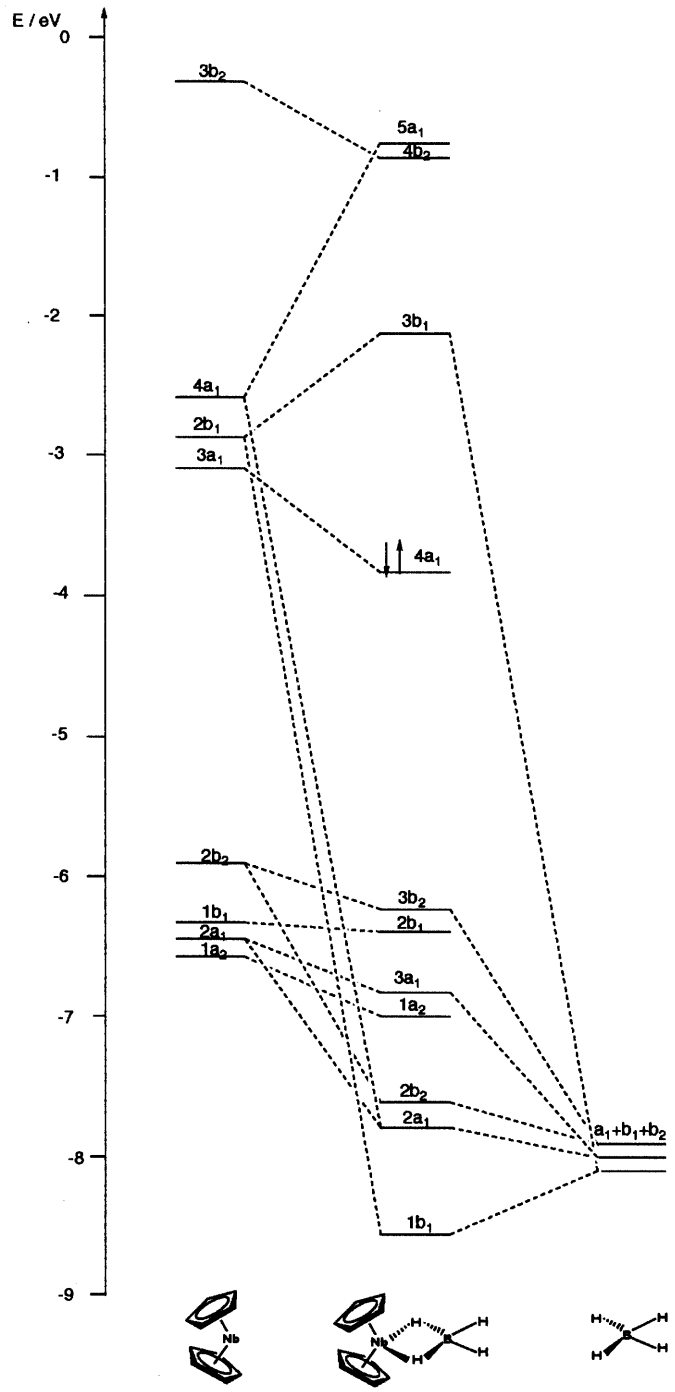

Fig. 2. MO scheme for $[Nb(\eta\text{-}C_5H_5)_2(\eta^2\text{-}BH_4)]$.

for the C-bridged compound. Whether the binding in the transition state is described as η^1 or η^3 is to a certain extent a matter of semantics, but it should be noted that both these nomenclatures imply a local C_3 axis for the $NbBH_4$ unit and the proposed transition state clearly lacks that.

Location of a mid-point for pathway 2 proved less simple. A similar procedure imposing C_s symmetry with this time yz as the mirror plane always reverted to the ground state structure. A linear transit run where the BH_4 group was rotated to bring H_a in to the yz plane led through the transition state found previously to the ground state structure with H_a exchanging with H_c.

3.3. Bonding considerations

A metallocene fragment presents three frontier orbitals for binding in the xz plane, two of a_1 and one of b_1 symmetry. These are numbered $3a_1$, $2b_1$ and $4a_1$ to be consistent with a recent review [2]. Fig. 2 shows a MO diagram for the ground state of **1a**. This was constructed from $[Nb(\eta\text{-}C_5H_5)_2]$ and $[BH_4]$ fragments. The highest occupied orbital (HOMO) of a_1 symmetry is d_x^2 in character. Below the HOMO lie four orbitals with their principal origin in the bent metallocene fragment, being largely cyclopentadienyl in character. These are followed by three orbitals of mainly B–H origin. The highest of the three is of b_2 symmetry, largely localised on the terminal hydrogens and is not involved in Nb BH_4 binding. The lower pair both have a_1 and b_1 symmetry and some metal character; they are the two orbitals which bind the BH_4 unit to the metallocene fragment. The interactions are shown in Fig. 3(a) and (b).

Population analyses of the metallocene and borohydride frontier orbitals in the three compounds enables a comparison of bonding in the ground state structures. Gross populations of the metallocene $3a_1$, $2b_1$ $4a_1$ and $3b_2$ orbitals and the borohydride $2a_1$, $1b_1$ and $1b_2$

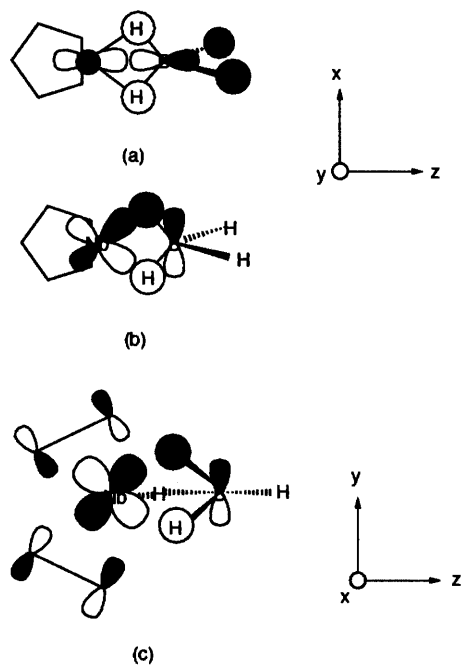

Fig. 3. Representations of bonding interactions in $[Nb(\eta\text{-}C_5H_5)_2(\eta^2\text{-}BH_4)]$: (a) Nb–$BH_4$ a_1 ground state interaction; (b) Nb–BH_4 b_1 ground state interaction; (c) Nb–BH_4 a'' transition state interaction.

Table 3
Gross occupancies of metallocene (MCp_2) and BH_4 frontier orbitals in **1a**, **2a** and **3a** in their η^2 ground state (gs) and in the proposed transition states (ts)

	1a (gs)	**2a** (gs)	**3a** (gs)	**1a** (ts)	**2a** (ts)	**3a** (ts)
Mcp_2						
$3b_2$	0.03	0.03	0.05	0.12	0.14	0.17
$4a_1$	0.36	0.24	0.18	0.22	0.16	0.12
$2b_1$	0.36	0.35	0.31	0.32	0.32	0.30
$3a_1$	1.83	1.86	1.89	1.86	1.86	1.88
BH_4						
$2a_1$	1.71	1.78	1.82	1.81	1.82	1.85
$1b_1$	1.65	1.67	1.71	1.70	1.72	1.72
$1b_2$	1.92	1.91	1.89	1.85	1.84	1.81

orbitals are given in Table 3. The borohydride orbitals are those descended from the t_2 bonding orbitals of a tetrahedral BH_4 group. In a metallocene cation $3a_1$ would have an occupancy of 2, as would all three BH_4 frontier orbitals in a tetrahydroborato anion. Thus the degree of departure from occupancies of either 2 or 0 give the amount of covalent mixing. In all cases there is more mixing in the b_1 interaction than the a_1. This fits with the $4a_1$ orbital of the metallocene fragment being higher in energy than the $2b_1$. The largest change along the series is the a_1 interaction, which decreases with increasing ring angle, α. Again the $4a_1$ metallocene orbital rises most with increase in α. The b_1 interaction also decreases with increase in α but not by so much, the $2b_1$ fragment orbital being less sensitive to the degree of bending of the metallocene unit. The weaker metal borohydride interactions in **3a** are consistent with the longer Nb–$H_{a,b}$ and Nb…B distance calculated for the carbon bridged compound. Thus the BH_4 unit becomes more weakly bound with increase in inter-ring angle. IR stretching frequencies confirm this; as α increases ν_{av} (B–H (bridging)) increases [6].

A comparison is also possible between the bonding in the proposed transition states. The structure is such that H_b and H_c lie above and below the xz plane and approach the metal sufficiently to interact with the metal d_{yz} orbital (Fig. 3(c)). This may be envisaged as donation from BH_4 into the high lying $3b_2$ orbital. This latter orbital is not normally considered as a 'frontier' orbital in a metallocene unit as it lies high in energy having its parentage in one of the anti-bonding e_1'' orbitals of the parallel metallocene. The metal-ring anti-bonding nature is depicted in Fig. 3(c). As α increases the $3b_2$ orbital drops in energy. Thus it is to be expected that it is most available to **3a** which has the largest α. The gross occupancies of the fragments in the three transition states given in Table 3 show this to be the case with **3a** having the highest degree of mixing between the b_2 orbitals. It is also the case that **3a** having the lowest a_1 and b_1 in the ground state suffers less loss of this mixing on going to the transition state than the other two compounds. Thus the transition state becomes more easily accessible with increase in α.

4. Conclusions

Density functional calculations on **1a**, **2a** and **3a** identify a transition state for terminal bridging H exchange where the two exchanging hydrogens lie above and below the inter-ring plane. The energy of this transition state relative to the ground state decreases with inter-ring angle. The calculated energy differences are close in value to the free energies of activation for the exchange in **1a**, **2b** and **3b** determined by ^{1}H-NMR. Examination of the ground state electronic structures suggests that covalent Nb–BH_4 bonding decreases with an increase in the inter-ring angle. Also a greater bending of the rings increases binding in the transition state. Both effects contribute to the lowering of the energy barrier.

Acknowledgements

We thank the EPSRC for a studentship (SLJC). Part of this work was carried out using the resources of the Oxford Supercomputing Centre.

References

[1] J.A. Smith, H.H. Brintzinger, J. Organomet. Chem. 1981 (1981) 158.
[2] J.C. Green, Chem. Soc. Rev. (1998) 263 and references therein.
[3] S.L.J. Conway, T. Dijkstra, L.H. Doerrer, J.C. Green, M.L.H. Green, J. Chem. Soc. Dalton Trans. (1998) 2689.
[4] D. Churchill, J.H. Shin, T. Hascall, J.M. Hahn, B.M. Bridgewater, G. Parkin, Organometallics 18 (1999) 2403.
[5] A. Chernega, J. Cook, M.L.H. Green, L. Labella, S.J. Simpson, A.H.H. Stephens, J. Chem. Soc. Dalton Trans. (1997) 3225.
[6] S.L.J. Conway, L.H. Doerrer, M.L.H. Green, M.A. Leech, J. Chem. Soc. Dalton Trans. (2000) 630.

[7] J.C. Green, C.N. Jardine, J. Chem. Soc. Dalton Trans. (1998) 1057.
[8] J.C. Green, A. Scottow, New J. Chem. 23 (1999) 651.
[9] J.C. Green, C.N. Jardine, J. Chem. Soc. Dalton Trans. (1999) 3767.
[10] E.J. Baerends, G. te Velde, ADF 2.3.0, Theoretical Chemistry, Vrije Universiteit, Amsterdam, 1997.
[11] ADF Program System Release 1999, E.J. Baerends, A. Berces, C. Bo, P.M. Boerringter, L. Cavallo, L. Deng, R.M. Dickson, D.E. Ellis, L. Fan, T.H. Fischer, C. Fonseca Guerra, S.J. van Gisbergen, J.A. Groeneveld, O.V. Gritsenko, F.E. Harris, P. van den Hoek, H. Jacobsen, G. van Kessel, F. Kootstra, E. van Lenthe, V.P. Osinga, P.H.T. Philipsen, D. Post, C.C. Pye, W. Ravenek, P. Ros, P.R.T. Schipper, G. Schreckenbach, J.G. Snijiders, M. Sola, D. Swerhone, G. te Velde, P. Vernooijis, L. Versluis, O. Visser, E. van Wezenbeek, G. Wiesenekker, S.K. Wolff, T.K. Woo, T. Ziegler, 1999
[12] S.H. Vosko, L. Wilk, M. Nusair, Can. J. Phys. 58 (1980) 1200.
[13] A.D. Becke, Phys. Rev. Sect. A 38 (1988) 2398.
[14] J.P. Perdew, Phys. Rev. Sect. B 33 (1986) 8822.
[15] J.P. Perdew, Phys. Rev. Sect. B 34 (1986) 7046.
[16] N.I. Kurillova, A.I. Gusev, Y.T. Struchov, Zh. Strukt. Khim. 15 (1974) 718.
[17] M.L.H. Green, L.-L. Wong, J. Chem. Soc. Dalton Trans. (1989) 2133.